Natural hexavalent chromium in groundwaters interacting with ophiolitic rocks

Donatella Fantoni · Gianpiero Brozzo · Marco Canepa · Francesco Cipolli
Luigi Marini · Giulio Ottonello · Marino Vetuschi Zuccolini

Abstract Thirty of the 58 groundwaters sampled in September–October 2000 in the study area (La Spezia Province, Italy) have Mg–HCO_3 to Ca–HCO_3 composition, undetectable Cr(III) contents, and virtually equal concentrations of total dissolved Cr and Cr(VI). Therefore, dissolved Cr is present in toto as Cr(VI), with concentrations of 5–73 ppb. These values are above the maximum permissible level for drinking waters (5 ppb). Local ophiolites, especially serpentinites and ultramafites, are Cr-rich and represent a Cr source for groundwaters. However, since Cr is present as Cr(III) in rock-forming minerals, its release to the aqueous solution requires oxidation of Cr(III) to Cr(VI). This can be performed by different electron acceptors, including Mn oxides, H_2O_2, gaseous O_2, and perhaps Fe(III) oxyhydroxides. Based on this evidence and due to the absence of anthropogenic Cr sources, the comparatively high Cr(VI) concentrations measured in the waters of the study area are attributed to natural pollution.

Keywords Groundwater · Chromium · Hexavalent chromium · Ophiolites · Liguria

Introduction

In natural environments Cr is chiefly present in two oxidation states: Cr(III) and Cr(VI). Hexavalent Cr is comparatively mobile and highly toxic for humans upon inhalation and ingestion, whereas Cr(III) is almost immobile in most natural conditions and has low toxicity. Taking into account these distinct properties of the two main oxidation states of Cr, the Italian regulation (D.M. 25 October 1999, no. 471) imposed a maximum acceptable concentration of only 2 ppm (on a dry basis) for Cr(VI) in soils for private and residential use, against a limit of 150 ppm for total Cr. The same applies to groundwaters, with a maximum acceptable concentration of only 5 ppb for Cr(VI), which is 10 times lower than that for total Cr. Dissolved Cr reaches concentrations of some g kg^{-1} due to anthropogenic pollution, which is generally linked to the use of Cr(VI) compounds in several industrial applications such as plating, metallurgy, pigments, and leather tanning (e.g., Nriagu 1988).

The distribution of total Cr in natural groundwaters was investigated by Barnes and Langmuir (1978). They found total Cr thresholds, corresponding to the 97.7 percentile, of 10–19 ppb for 647 groundwaters associated with carbonate rocks, sandstones (including quartzites, arkoses, greywackes, and conglomerates), shales (comprising clays, siltstones, and slates), and felsic to intermediate igneous and meta-igneous rocks. By contrast, a total Cr threshold of 32 ppb was found for 35 groundwaters coming from mafic and ultramafic igneous and meta-igneous rocks. These distinct thresholds in the aqueous phase reflect the different concentrations in rocks. In fact, the worldwide average Cr contents of peridotites and basalts (1,800 and 185 ppm, respectively) are much higher than those of limestones (11 ppm), granites (22 ppm), sandstones (35 ppm), and shales (90 ppm; Faure 1992). However, these data are insufficient to define the natural (background) concentrations of Cr(VI) and Cr(III) in waters, a facet of utmost importance due to their different toxicity. Concentrations of Cr(VI) reaching 12 ppb and of Cr(III) reaching 11 ppb were recently found in groundwaters interacting with ultramafites (Robles-Camacho and Armienta 2000), indicating that these lithotypes may cause natural pollution of waters in not only Cr(III) but also Cr(VI).

Ultramafic rocks, usually affected by extensive serpentinization, are present in the La Spezia province (Fig. 1), and high Cr concentrations in some drinking waters interacting with these lithotypes were detected by the local Environmental Protection Agency. Based on this information, we decided to carry out a systematic study of the

Received: 1 October 2001 / Accepted: 8 April 2002
Published online: 4 June 2002

D. Fantoni · M. Canepa · F. Cipolli · L. Marini (✉)
G. Ottonello · M.V. Zuccolini
Department for the Study of the
Territory & its Resources, Genoa University,
Corso Europa 26, 16132 Genoa, Italy
E-mail: lmarini@hpe35.dipteris.unige.it

G. Brozzo
ACAM, via Alberto Picco 22,
19124 La Spezia, Italy

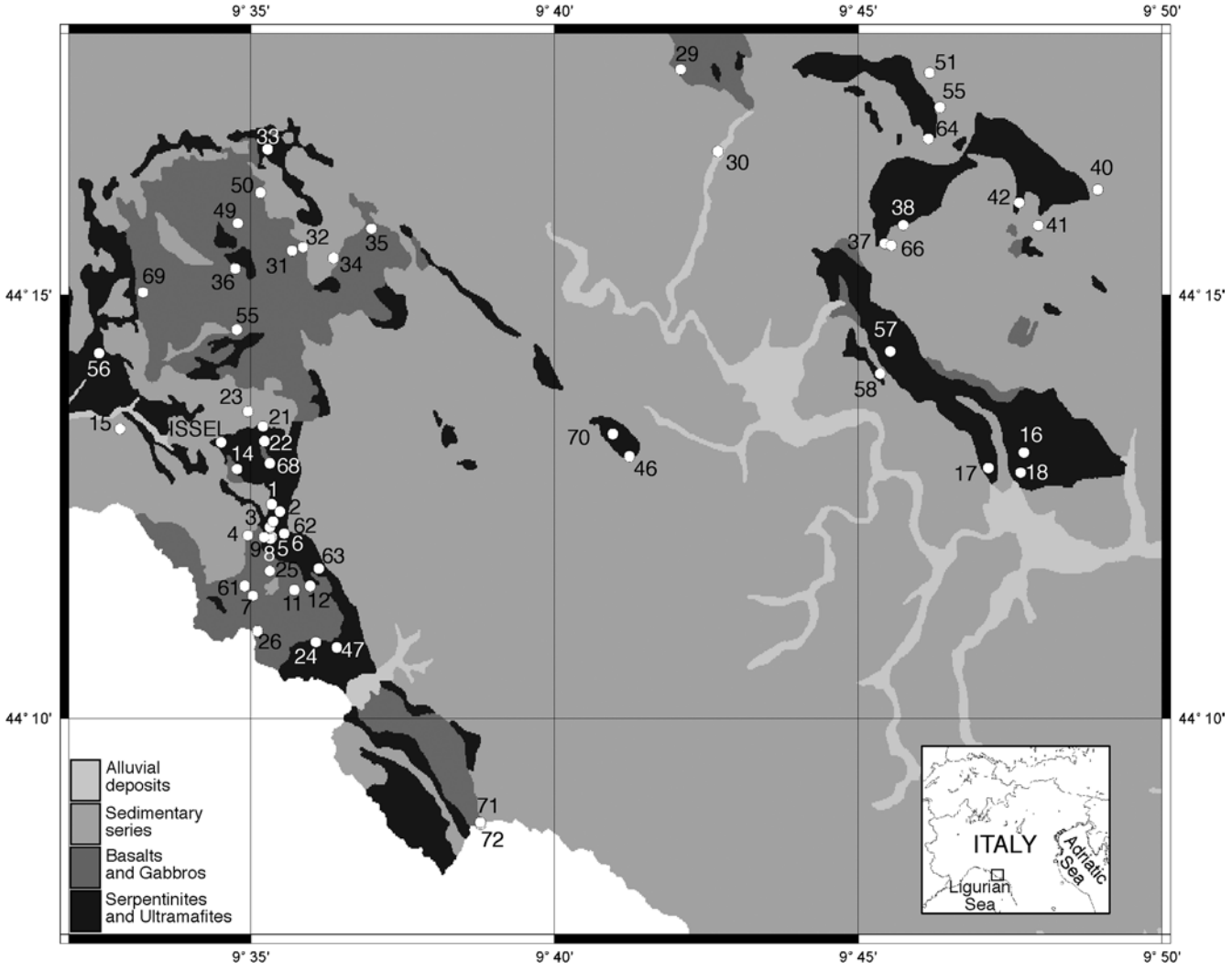

Fig. 1
Simplified geologic map of the study area (modified from sheet 95 La Spezia of the geological map of Italy), also showing the location of the sampled springs and shallow wells

groundwaters of the La Spezia province interacting with serpentinites and other ophiolitic rocks, aimed at defining the distribution and fate of both Cr(III) and Cr(VI) in these hydrogeological circuits.

Geological background

The ophiolitic rocks of the study area have been the subject of several geological and petrological investigations (e.g., Decandia and Elter 1972; Cortesogno and others 1978, 1980; Abbate and others 1980; Barret 1982; Cortesogno and others 1987). These authors recognized that these ophiolites were emplaced at the bottom of the Piedmontese-Ligurian oceanic basin belonging to the Western Tethys over 150 million years ago, in agreement with previous findings (Suess 1888, 1901; Steinmann 1905). Ophiolites, together with their sedimentary cover, were later involved in the Apenninic orogeny. The ophiolitic sequence comprises (1) the basement, consisting of prevailing ultramafites and subordinate gabbros, overlain by ophicalcites; (2) the volcano-sedimentary complex, made up of ophiolitic breccias and basalts, interbedded with sedimentary levels; and (3) the sedimentary cover comprising radiolarites and pelagic carbonates and shales.

Mineralogy of local ophiolites

The ultramafic rocks, chiefly lherzolites, are characterized by extensive alteration to serpentine minerals (chrysotile and lizardite), chlorites, and oxides. These substitute the primary mineralogical paragenesis, which is made up of olivine, orthopyroxene, clinopyroxene, spinel, and plagioclase. The gabbroic complex comprises ultramafic cumulates (dunites and rare plagioclase-bearing wherlites), Mg-gabbros, Fe-gabbros, and plagiogranites. The Mg-gabbros are the dominant lithotypes of the gabbroic complex and vary in composition from clinopyroxene-gabbros to olivine-gabbros and troctolites.
The weathering of serpentinites and ultramafic rocks of the Northern Apennines and Western Alps has been the subject of many studies (Bini and others 1990a, 1990b; Angelone and others 1991; Vaselli and others 1993;

De Siena and Vaselli 1994; Dinelli and others 1997; Venturelli and others 1997; Pfeifer and others 1999). Weathering of serpentinites initially determines the production of saponites and swelling chlorites (Bini and others 1990a, 1990b). Other weathering products are smectites and Fe oxides and hydroxides (Vaselli and others 1993; Venturelli and others 1997). In addition, secondary minerals forming at low temperatures include sepiolite (Caillère and Henin 1949; Wollast and others 1968), brucite (Hostetler and others 1966), and several carbonates such as calcite, aragonite, hydromagnesite, nesquehonite, and protodolomite (Barnes and O'Neil 1969; Suarez and Simunek 1996; Bruni and others 2001, 2002).

Field and laboratory work

Groundwaters interacting with ophiolitic rocks were sampled twice, in May–June 2000 and September–October of the same year, from 54 springs and four shallow wells. Intrinsically unstable parameters (i.e., temperature, pH, Eh, and alkalinity) were measured in the field by means of portable equipment, and flow rate was obtained by the speed × section method. Water was filtered through 0.45-μm membranes. A raw portion was stored, and a separate portion was acidified by addition of concentrated HNO_3 and stored. New polyethylene containers were utilized. The following chemical analyses were performed within a few days of sampling: (1) Li, Na, K, Mg, Ca, Al, Cr, Mn, Fe, Ni, Cu, and Zn by AAS; (2) F, Cl, SO_4, NO_3 by IC; (3) SiO_2, NO_2, NH_4, and PO_4 by visible spectrophotometry. The samples collected during the autumn survey were also analyzed for (1) hexavalent Cr by means of the 1,5-diphenylcarbohydrazide colorimetric method, and (2) trivalent Cr by ICP-OES, after pre-concentration through treatment with the cation exchange resin Dowex 50WX8. Relevant analytical data of the second sampling campaign are reported in Table 1, whereas the locations of sampled springs and shallow wells are shown in Fig. 1.

Hydrogeological observations

Sampled springs issue from fractured ophiolitic rocks and are located either near the contact with geological formations of relatively low permeability or along fractures and faults. In the geological framework of the investigated area, the main aquifers are hosted into serpentinites and subordinately into gabbros, basalts, and ophicalcites. Flow rates typically ranged from <0.5 to 2 l s^{-1} during the spring survey, and from 0.5 to 5 l s^{-1} during the autumn campaign. The four boreholes sampled during this study (samples 26, 62, 71 and 72 in Fig. 1 and Table 1) have productivity ranging between 1 and 4 l s^{-1}. Most surveyed springs and all the sampled boreholes are used for drinking-water supply.

Water chemistry

Apart from the sulfide-bearing Issel spring, other sampled waters have average pH of 7.64±0.38 (1 σ), average Eh of +188±65 mV, and average temperature of 12.6±1.7 °C. Water temperatures are close to the seasonal average air temperature at ground level. Most waters have either Ca–HCO_3 or Mg–HCO_3 compositions (Fig. 2), and the variation from Ca-rich to Mg-rich end members is continuous. The triangular plot of Mg, SiO_2, and HCO_3 (Fig. 3) is useful to distinguish Mg–HCO_3 and Ca–HCO_3 waters, and to investigate qualitatively the water-rock interaction processes affecting Mg–HCO_3 waters. The expected compositions of the aqueous phases produced by CO_2-driven dissolution of Mg-bearing solid phases are also reported in this plot. Theoretical compositions were computed assuming congruent dissolution of Al-free minerals, whereas incongruent dissolution accompanied by precipitation of kaolinite was hypothesized for Al-bearing minerals. All these theoretical compositions have a HCO_3/Mg molar ratio of 2, imposed by the electroneutrality constraint, and variable SiO_2/Mg and SiO_2/HCO_3 ratios, reflecting the stoichiometry of the different mineral phases. Calcium-HCO_3 waters have an HCO_3/Mg molar ratio greater than 2, since much of their dissolved HCO_3 is balanced by Ca ion. By contrast, magnesium-HCO_3 waters have HCO_3/Mg molar ratios close to 2 and plot slightly to the left of the serpentine point. This indicates that Mg–HCO_3 waters are produced through incongruent dissolution of serpentine, which is evidently accompanied by precipitation of phases richer in SiO_2 than serpentine. These solid products are most likely Mg-saponites and/or Mg-montmorillonites, in agreement with previous findings (Bruni and others 2001, 2002). Based on these findings and taking into account spring location and the geology of the study area, it seems likely that Ca–HCO_3 waters originate through the interaction of meteoric waters with rocks containing Ca minerals, chiefly gabbros and basalts, whereas Mg–HCO_3 waters are produced by dissolution of serpentinites and ultramafic rocks. The continuous variation from Ca-rich to Mg-rich compositions (Fig. 2) suggests either that many waters interact with both Ca-rich and Mg-rich rocks or that Ca–HCO_3 waters mix rather frequently with Mg–HCO_3 waters. In any case, no impermeable barriers evidently separate the gabbros and basalts from the ultramafic rocks.

The sulfide-bearing Issel spring has HCO_3–CO_3–OH–Na composition, pH 10.5, Eh –0.3 V, and temperature 14–15 °C. The characteristics of this spring are intermediate between those of shallow, immature Mg–HCO_3 waters and those of relatively deep, mature Ca–OH waters. High-pH Ca–OH waters, in fact, typically originate through prolonged interaction of meteoric waters and ultramafic rocks (Bruni and others 2001, 2002 and references therein).

The transfer of Cr from rocks to waters

Chromium contents and speciation in waters

The virtual absence of detectable Cr(III), whose concentration is below 1 ppb in all the samples of the autumn survey, and the good correspondence between Cr(VI) and

Table 1
Analytical data of groundwaters, showing the concentrations of chemical constituents (in mg kg^{-1}) and other relevant data for the water samples collected in the study area in September–October 2000. Total (titration) alkalinity (*Alk*) is in mg kg^{-1} HCO_3, *n.d.* Not detected, *n.a.* not analyzed

Sample	T (°C)	Eh (mV)	pH	Ca	Mg	Na	K	Alk	SO_4	Cl	NO_3	SiO_2	Cr(tot)	Cr(VI)
1	11.4	60	7.61	29.64	30.51	7.07	0.16	216.4	10.47	15.68	0.70	22.5	0.017	0.017
2	11.4	25	8.23	10.32	35.65	6.56	0.57	179.4	7.67	11.64	0.62	33.1	0.023	0.027
3	12.1	114	7.61	11.07	40.15	7.39	0.59	200.8	7.90	12.38	1.27	29.6	0.022	0.020
4	13.8	148	7.97	27.12	6.03	8.72	0.42	94.6	6.60	12.78	0.68	4.3	0.005	n.d.
5	12.5	161	7.84	9.87	36.44	12.19	0.58	207.5	5.87	12.78	0.54	42.3	0.060	0.060
6	13.0	170	7.97	13.01	35.77	7.31	1.32	196.5	7.03	14.13	0.00	30.6	0.073	0.073
7	14.9	150	7.67	29.75	21.24	14.40	1.17	156.8	19.09	17.96	10.35	19.2	0.005	n.d.
8	13.2	165	7.58	10.88	38.03	10.79	0.24	212.4	6.03	12.53	0.37	31.1	0.044	0.042
9	13.0	193	7.87	14.18	37.76	7.61	0.55	219.7	7.25	12.29	0.86	27.5	0.025	0.021
11	14.4	102	7.80	24.48	19.16	12.66	0.73	140.4	17.76	16.70	0.00	19.4	n.d.	n.d.
12	13.6	149	8.60	20.37	69.72	9.02	0.96	295.3	65.89	21.79	0.09	34.6	n.d.	n.d.
Issel	14.7	–288	10.51	4.02	4.00	33.79	1.97	75.7	24.31	8.33	0.13	10.1	n.d.	n.d.
14	13.0	195	8.15	12.89	33.67	11.71	0.68	187.9	17.89	11.47	0.18	15.0	0.005	n.d.
15	13.4	168	7.60	65.76	14.41	11.50	1.10	218.5	23.89	15.04	1.50	8.0	n.d.	n.d.
16	13.7	105	7.62	3.17	33.77	4.00	0.28	159.9	5.83	7.26	0.23	35.4	0.019	0.016
17	14.0	150	7.54	51.99	35.93	5.81	0.35	294.7	11.67	12.74	0.00	49.0	0.036	0.036
18	14.8	–95	8.10	7.62	36.23	6.54	0.28	181.2	7.58	13.16	0.00	34.9	0.013	0.012
21	11.4	108	7.47	6.04	32.34	5.43	0.27	153.8	10.05	10.99	0.74	32.0	0.034	0.034
22	11.5	153	7.27	5.71	23.59	6.53	0.27	117.8	8.52	9.91	0.36	24.3	0.035	0.034
23	12.1	139	7.56	59.11	6.14	9.23	0.86	164.8	15.39	17.71	2.24	14.4	n.d.	n.d.
24	15.8	105	7.44	26.38	14.70	10.77	0.30	128.1	14.46	16.59	4.10	12.6	0.006	n.d.
25	14.2	146	7.63	41.16	34.77	13.48	1.28	252.6	20.01	23.94	6.22	35.2	0.016	0.014
26	15.7	107	7.01	71.25	59.22	136.30	7.15	372.8	60.04	198.55	8.45	30.8	0.007	n.d.
28	12.9	221	7.56	71.57	6.87	7.70	0.97	299.4	13.82	9.21	0.83	10.4	0.009	0.009
29	10.6	228	7.26	20.41	8.87	6.25	0.79	115.3	6.77	5.17	0.36	13.9	0.005	n.d.
30	11.6	145	7.61	21.92	12.30	6.89	0.27	112.9	10.48	7.11	0.20	15.1	n.d.	n.d.
31	11.0	227	7.49	22.30	8.18	6.23	0.35	100.7	3.74	7.19	0.05	15.7	0.016	0.016
32	11.2	219	7.53	29.13	6.40	6.33	0.61	115.3	4.42	7.49	0.38	18.8	0.014	0.014
33	12.1	211	7.52	23.48	6.38	5.68	0.32	88.5	8.23	6.41	1.02	15.9	n.d.	n.d.
34	12.8	222	7.43	38.66	10.29	8.90	0.68	161.7	10.32	7.92	0.10	23.0	0.005	n.d.
35	12.1	215	7.44	73.94	5.30	7.50	0.79	223.3	12.41	8.72	0.37	14.0	n.d.	n.d.
36	10.9	224	7.19	21.90	7.31	6.23	0.24	80.6	17.52	8.11	0.46	13.7	n.d.	n.d.
37	11.5	499	7.58	24.90	26.34	5.92	0.63	174.5	12.50	6.82	2.04	29.5	0.031	0.030
38	11.2	179	7.83	49.19	17.45	6.08	0.82	200.8	16.58	6.90	1.68	19.1	0.012	0.012
40	10.1	219	7.55	75.85	7.32	4.50	0.33	231.9	8.37	6.53	1.26	16.7	n.d.	n.d.
41	10.6	182	7.76	55.39	6.75	4.81	0.51	181.8	11.28	6.11	1.96	11.4	n.d.	n.d.
42	12.3	141	8.34	16.38	16.10	3.77	0.25	117.2	5.55	5.71	0.85	15.7	0.008	n.d.
46	12.7	146	7.41	4.97	37.54	5.20	0.67	170.3	10.71	7.83	1.48	36.2	0.072	0.072
47	15.4	164	8.00	37.06	49.44	11.56	0.82	281.9	31.85	28.45	3.38	50.1	0.024	0.023
49	11.3	191	7.33	12.72	4.38	7.01	0.13	53.7	13.25	7.79	0.92	10.2	n.d.	n.d.
50	11.9	195	7.44	26.71	11.10	6.97	0.27	126.3	8.65	6.88	0.67	14.6	n.d.	n.d.
51	11.2	223	7.70	49.17	8.09	5.88	0.86	150.7	28.95	5.39	4.03	10.4	n.d.	n.d.
55	12.5	199	7.36	25.70	13.48	9.55	0.29	115.3	19.38	15.11	2.62	16.4	0.006	n.d.
56	13.9	205	7.58	59.62	16.00	7.59	0.80	230.7	10.39	15.25	0.87	24.5	0.023	0.021
57	13.4	130	7.98	6.94	45.26	5.37	0.36	213.6	14.78	8.70	0.26	35.9	n.d.	n.d.
58	14.0	115	8.00	11.74	45.25	12.19	0.29	231.3	17.73	8.96	1.09	42.3	n.d.	n.d.
61	14.4	139	7.82	28.54	19.90	13.92	1.22	148.9	16.96	17.45	8.51	29.9	n.d.	n.d.
62	12.7	n.a.	8.12	11.61	39.70	5.86	0.30	209.3	9.68	12.71	0.46	29.2	0.024	0.024
63	13.3	130	7.95	32.61	33.61	8.47	0.54	231.9	4.98	16.34	1.04	42.1	0.032	0.030
64	11.2	198	7.89	12.35	21.41	3.38	0.31	121.4	9.68	5.95	2.86	19.5	0.021	0.021
65	13.2	111	7.47	63.68	8.83	5.86	1.55	180.6	32.19	6.14	2.41	22.0	n.d.	n.d.
66	11.6	321	7.85	21.80	24.64	5.84	0.65	164.8	10.52	6.91	1.51	24.7	0.033	0.033
67	11.3	210	7.90	8.42	15.62	3.05	0.22	94.6	5.57	4.63	0.62	16.6	0.017	0.017
68	12.7	178	7.91	10.54	22.77	8.33	0.26	123.3	13.20	13.37	0.08	19.7	0.019	0.019
69	15.7	115	8.05	22.06	14.88	11.18	0.28	111.1	15.11	15.55	0.53	16.5	n.d.	n.d.
70	12.7	190	8.07	2.69	31.91	4.11	0.18	150.1	4.51	6.95	0.46	32.0	n.d.	n.d.
71	17.2	n.a.	7.20	52.47	37.41	38.26	0.83	286.8	36.06	43.24	13.50	n.a.	n.d.	n.d.
72	18.3	n.a.	7.20	43.97	39.70	50.67	1.26	302.7	44.47	39.23	17.71	n.a.	n.d.	n.d.

total Cr contents (Fig. 4) indicate that dissolved Cr is essentially present in toto in the hexavalent form. In 30 of the 58 sampled waters (52% of the data set), Cr(VI) content is above the maximum permissible level for drinking waters of 5 ppb.

Chromium speciation indicated by analytical data is at variance with equilibrium speciation computed by means of the EQ3NR software code (Wolery 1992). According to equilibium-speciation calculations, at the average Eh (188 mV), pH (7.64), and temperature (12.6 °C) of

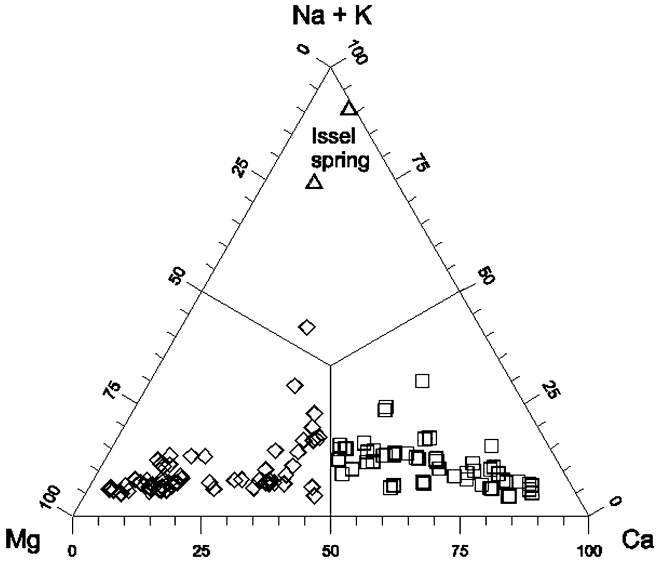

Fig. 2
Ca–Mg–(Na–K) triangular plot for the waters of the study area, computed from concentrations in meq l^{-1}. *Diamonds* Mg–HCO_3 waters, *squares* Ca–HCO_3 waters, *triangles* sulfide-bearing Issel spring, of HCO_3–CO_3–OH–Na composition

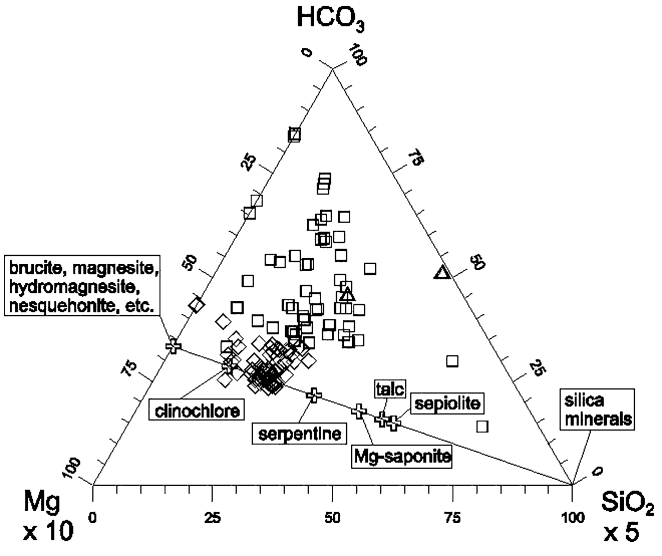

Fig. 3
Mg–SiO_2–HCO_3 triangular plot for the waters of the study area, computed from concentrations in mg l^{-1}. *Diamonds* Mg–HCO_3 waters, *squares* Ca–HCO_3 waters, *triangles* sulfide-bearing Issel spring, of HCO_3–CO_3–OH–Na composition. Also shown (*crosses*) are the expected compositions of the aqueous phase controlled by CO_2-driven dissolution of Mg-bearing solid phases

Ca–HCO_3 and Mg–HCO_3 waters, dissolved Cr is totally present in the trivalent form and the main aqueous species are $Cr(OH)_2^+$ and $Cr(OH)_3$, which account for 82 and 17% of total dissolved Cr, respectively. The computed concentration of Cr(VI) is 10 orders of magnitude lower than that of Cr(III). This discrepancy between analytical data and equilibrium Cr speciation indicates the existence of redox disequilibrium between Cr species and the redox couple governing measured Eh values, if any.

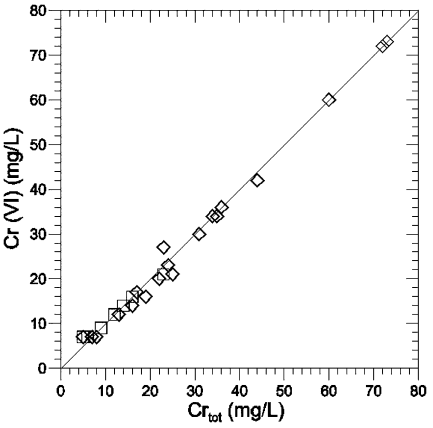

Fig. 4
Correlation plot of Cr(VI) vs. total dissolved Cr for the waters of the study area

Not surprisingly, analytical Cr distribution in groundwaters is correlated with water chemistry. Ten Ca–HCO_3 waters (48% of this group) have detectable Cr concentrations (≥5 ppb; maximum 23 ppb), whereas Cr is undetectable in the remaining 11 samples. Magnesium-HCO_3 waters comprise 20 samples (83% of this group) with measurable Cr concentrations (maximum 73 ppb), and four samples with less than 5 ppb Cr. The different Cr distributions in these two groups of groundwaters likely reflect, at least in part, the distinct Cr concentrations of rocks. Interestingly, the maximum Cr content in the surveyed groundwaters is about half the maximum value reported for underground waters from the Hinokami chromite ore district in Japan (134 ppb; Yamagata and others 1960).

Chromium in rocks and minerals

The minimum, average, and maximum Cr contents in stream sediments from Ligurian catchments dominated by ultramafic rocks are 684, 1,370, and 2,740 ppm, respectively (Ottonello 2001a). This mean value is somewhat lower than the average worldwide Cr content of peridotites (1,800 ppm; Faure 1992), possibly because of the presence of rocks poorer in Cr, such as basalts and gabbros. Chromium distribution in rock-forming minerals was summarized by Deer and others (1975) and Wedepohl (1978). Among the minerals of the spinel group, high Cr concentrations are found not only in chromite and magnesio-chromite but also in other members, such as magnetite which is a generally abundant constituent of ultramafites. Olivines are usually very poor in Cr (<70 ppm), and high Cr contents in former analyses are likely due to tiny inclusions of Cr-rich spinel. The Cr content of pyroxenes is generally lower than 2%, with clinopyroxene usually containing more Cr than the coexisting orthopyroxene. Typical Cr contents in serpentine are ~100 ppm.

The oxidative dissolution of Cr

According to Robles-Camacho and Armienta (2000) the chromite edges, mostly made up of magnetite, are the first

to dissolve. Chromium release could also derive from dissolution of the magnetite which is typically present at the edges of olivine and pyroxenes, as well as between serpentine fibers. These Cr-rich solid phases are among the main rock-forming minerals of the lithotypes present in the study area, and their dissolution evidently releases comparatively high amounts of Cr to waters.

In any case, whatever the solid sources of Cr are, this element is present in the trivalent state in all these mineral phases. Therefore, the release of Cr to the aqueous solution requires oxidation of Cr(III) to Cr(VI), at least in the groundwaters under study. In principle, the possible electron acceptors include Mn oxides, Fe(III) oxyhydroxides, H_2O_2, dissolved O_2, and gaseous O_2. Mn oxides are able to oxidize Cr(III), as expressed by the following reaction,

$$Cr(OH)^{2+} + 1.5MnO_2 = HCrO_4^- + 1.5Mn^{2+}, \quad (1)$$

which proceeds relatively fast (Raphael and Boulis 1982; Eary and Rai 1987; Saleh and others 1989; Johnson and Xyla 1991; Fendorf and Zasoski 1992).

According to Fendorf (1995), the Mn oxides are the only possible electron acceptors involved in Cr(III) oxidation, but the picture may be more complicated. The possible role of Fe(III) oxyhydroxides, which are produced through magnetite decomposition, deserves further investigation. Hydrogen peroxide is a strong oxidant and the rate of the H_2O_2-driven Cr(III) oxidation to Cr(VI) is fast (Pettine and Millero 1990). For an H_2O_2 concentration of 26×10^{-6} mole l^{-1}(a reasonable value for rainwaters of oceanic regions; Yuan and Shiller 2000), a pH of 6 (a common value for rainwaters not affected by strongly acid gases and suspended solid particles), and a temperature 15°C, the half-life of the Cr(III) oxidation to Cr(VI) is approx. 4.6 days, based on the relationship by Pettine and Millero (1990). The role of dissolved O_2 is probably subordinate. In fact, studies on the oxidation kinetics of Cr(III) to Cr(VI) driven by dissolved O_2 in seawater have shown that this is a rather sluggish process which cannot explain the high Cr(VI) concentrations in seawater (Fukai and Vas 1969; Schroeder and Lee 1975; Cranston and Murray 1978; Emerson and others 1979). Gaseous O_2 of the atmosphere could oxidize the trivalent Cr of Cr-rich spinels upon forest burning, a rather frequent event in the study area. This natural process mimics the high-temperature, O_2-driven oxidation of chromite to sodium chromate,

$$2FeCr_2O_4 + 4Na_2CO_3 + 7/2O_2 = 4Na_2CrO_4 + Fe_2O_3 + 4CO_2, \quad (2)$$

which is carried out in industrial chemical plants for chromate production.

Summing up, in the study area there are both a source of Cr(III), represented by the ultramafic rocks variably affected by serpentinization, and different electron acceptors (Mn oxides, H_2O_2, gaseous O_2, and perhaps Fe(III) oxyhydroxides) potentially able to promote oxidation of Cr(III) to Cr(VI). Based on this evidence and on the absence of anthropogenic Cr sources, the relatively high Cr(VI) concentrations observed in the waters of the study area can be attributed to natural pollution.

The fate of Cr during water-rock interaction

In order to investigate the fate of Cr during water-rock interaction, it is necessary to take into account the mineral phases possibly acting as stable Cr sinks. Note that adsorption processes on solid surfaces are neglected in this investigation. Surface adsorption processes represent, in fact, temporary buffers, which may explain the retardation in the transport of a given pollutant mass introduced into the groundwater flow by a discrete event. From our point of view, this is a negligible second-order effect, and attention is concentrated rather on the solid products of water-rock interaction, which can permanently incorporate Cr(III) in their lattices. These product phases are the Fe(III)-rich hydroxides and clay minerals, mainly saponites and montmorillonites, based on the geological setting of the study area, the weathering effects on serpentinites and ultramafites (see above), and the results of geochemical modeling (Bruni and others 2001, 2002).

Updating the thermodynamic database

To make the simulation sufficiently realistic, it was not limited to Cr(III), Cr(VI) and the major components, but Mn(II), Mn(III), Fe(II), Fe(III), and Ni were included as well. The thermodynamic data of the hydroxides of transition metals are known, whereas the thermodynamic data of saponites and montmorillonites are available only for the Na, K, Cs, Mg, Ca, and protonated end members. Following Sverjensky (1984, 1985), the Gibbs free energies of formation of unknown components of montmorillonites and saponites (at 25 °C, 1 bar) were obtained from empirical correlations between the Gibbs free energy of formation of the known end members, $\Delta G^\circ_{f,\ min}$, and the Gibbs free energy of formation of the related cations, $\Delta G^\circ_{f,\ ion}$, divided by the charge, Z. For montmorillonites, the following relationship was obtained (Fig. 5),

$$\Delta G^\circ_{f,\min} = -1248.99 + 0.3584\left(\Delta G^\circ_{f,ion}/Z\right) \quad (3)$$

whereas saponite data fit the equation

$$\Delta G^\circ_{f,\min} = -1321.62 + 0.3592\left(\Delta G^\circ_{f,ion}/Z\right). \quad (4)$$

Since saponites and montmorillonites of transition metals have Gibbs free energies of formation significantly higher than alkaline and alkaline-earth end members (Fig. 5), the incorporation of transition metals in their lattices is energetically unfavorable, and it is expected to be a minor process. The hydrolysis reactions of any montmorillonite is schematically represented as follows:

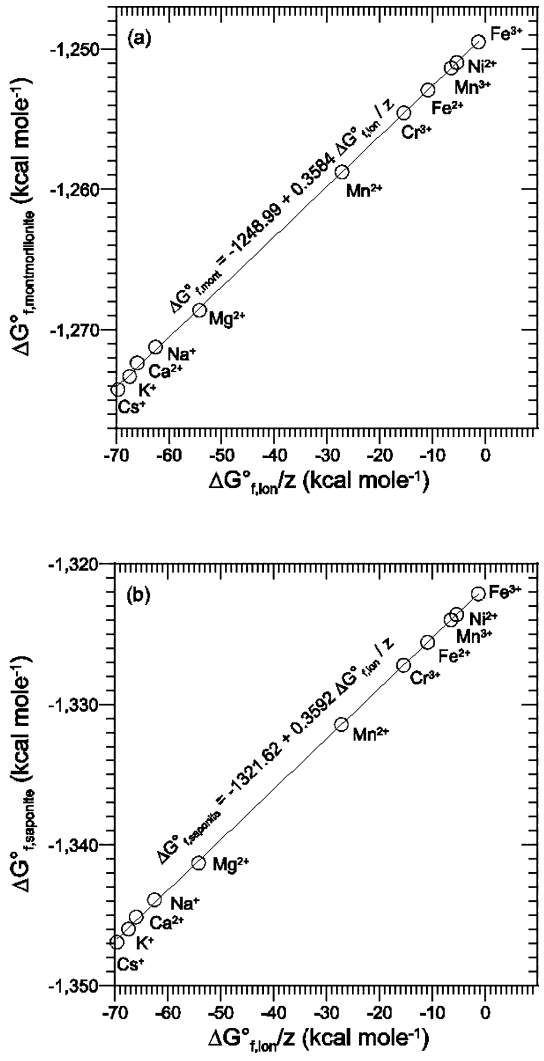

Fig. 5a, b
Correlation plot between the standard Gibbs free energy of formation of **a** saponites, and **b** montmorillonites, and the $\Delta G_{f,\ ion}/Z$ ratio, involving the Gibbs free energy of formation of the characterizing cations and their charges

$$\text{montmorillonite} - \text{M} + 6\text{H}^+ = \\ = (0.33/Z)M^{Z+} + 0.33\text{Mg}^{2+} + 1.67\text{Al}^{3+} + 4\text{SiO}_2 + 4\text{H}_2\text{O}, \quad (5)$$

where M^{Z+} represents the characterizing cation, and for any saponite we can write:

$$\text{saponite} - \text{M} + 7.32\text{H}^+ = \\ = (0.33/Z)M^{Z+} + 3\text{Mg}^{2+} + 0.33\text{Al}^{3+} + 3.67\text{SiO}_2 + 4.66\text{H}_2\text{O}. \quad (6)$$

Taking into account the stoichiometry of reactions (5) and (6), it is evident that the cation M^{Z+} contributes little to the Gibbs free energy of the hydrolysis reaction and to its thermodynamic constant, K. Consequently, the adopted polynomial functions describing the dependence of log K on temperature (where K_0 is the K value at 0 °C),

$$\log K = \log K_0 + BT + CT^2, \quad (7)$$

have very similar coefficients, especially for cations of the same charge. Based on the log *K* at 25 °C and taking average values for the *B* and *C* coefficients of Eq. (7), the log *K* values were computed at 0, 60, and 100 °C (Table 2). Estimated log *K* values for saponites and montmorillonites of transition metals were inserted in the thermodynamic database COM of the software package EQ3/6 (see below). This database contains the thermodynamic data of a large number of solids, aqueous species and gases, which were mainly derived from SUPCRT92 (Johnson and others 1992).

The water-rock interaction model

The water-rock interaction model represents an extension of that of Bruni and others (2001, 2002), suitably modified to include not only the major components but also transition metals. The software package EQ3/6 version 7.2b (Wolery 1992; Wolery and Daveler 1992) was used and reaction-path modeling was carried out by referring to the reaction progress variable (Helgeson 1979 and references therein), with no time provision. This choice is dictated by the huge uncertainties in both reactive surface areas and dissolution-precipitation rates of relevant mineral phases. Freyssinet and Farah (2000) estimated the dissolution rate of serpentine in an Amazon watershed where ultramafic rocks crop out, by means of elemental mass balances at a watershed scale. The values obtained (either 2.8×10^{-14} or 3.3×10^{-16} mol Si m^{-2} s^{-1}, depending on the reactive surface area considered) differ from the laboratory result

Table 2
Hydrolysis constants for saponites and montmorillonites of transition metals. Coefficients of the polynomial function log K=logK_0+B T+C T^2 (T in °C), used to compute the logarithms of the hydrolysis constant, including the log K value at 0 °C, log K_0

Cation charge	B	C	T (°C)	Cr^{3+}	Fe^{2+}	Fe^{3+}	Ni^{2+}	Mn^{2+}	Mn^{3+}
Saponites									
+1	−0.1196	1.397E−04	0	30.46	30.37	30.77	30.49	30.02	30.65
+2	−0.1274	1.577E−04	25	27.19	27.29	27.50	27.40	26.94	27.38
+3	−0.1352	1.757E−04	60	22.98	23.30	23.29	23.41	22.95	23.17
			100	18.70	19.21	19.00	19.33	18.86	18.89
Montmorillonites									
+1	−0.04433	−8.064E−05	0	4.85	4.75	5.14	4.87	4.42	5.03
+2	−0.05230	−6.139E−05	25	3.31	3.40	3.61	3.52	3.07	3.50
+3	−0.06027	−4.213E−05	60	1.08	1.39	1.37	1.51	1.06	1.26
			100	−1.60	−1.09	−1.31	−0.98	−1.43	−1.42

(3.3×10^{-8} mol Si m^{-2} s^{-1}; Lin and Clemency 1981) by 6–8 orders of magnitude. This huge difference cannot be explained assuming a partial contact between mineral surfaces and aqueous solutions, as suggested by Svoboda-Goldberg and Drever (1992) and Velbel (1993). In addition, reactive surface areas and dissolution-precipitation rates of mineral phases can undergo large changes during water-rock interaction progress (Marini and others 2000; Ottonello 2001b).

Only the chemical composition of the solid reactant (i.e., any material of known stoichiometry, irrespective of its thermodynamic stability; Wolery and Daveler 1992) has to be specified when reaction-path modeling is carried out in the reaction progress mode. In this investigation, the same serpentinite as that of Bruni and others (2001, 2002) was used as special reactant (Table 3). However, it is not correct to assume bulk dissolution of the solid reactant, especially for Cr, which is largely concentrated in mineral phases of very low solubility such as chromite (see above). A possible way to circumvent this problem is suggested by the results of selective extraction experiments from ultramafic rocks and related soils in 0.05 M EDTA at pH 7 (Angelone and others 1991). These are compared with both total concentrations in rocks and measured concentrations in the groundwaters of the study area in the log-log plot of Cr vs. Mg shown in Fig. 6. Total Cr contents in rocks are at least two orders of magnitude higher than in EDTA solutions, and at least three orders of magnitude higher than in local groundwaters. However, Cr/Mg ratios in groundwaters and in EDTA solutions are comparable. Therefore, the Cr available for leaching was considered to be 1% of the total content of the serpentinite used as special reactant, as also indicated by Schlegel and Pfeifer (1999).

Reaction-path modeling was executed in titration mode, that is, at each step of the reaction progress variable a corresponding amount of serpentinite was added to the system comprising the aqueous solution and eventual product phases. The added serpentinite is dissolved and resulting product phases, if any, are re-equilibrated with the aqueous solution (Wolery and Daveler 1992). Some product phases have a typically ephemeral existence and are re-dissolved upon further progress of the process. Other product phases, with which the aqueous solution attains equilibrium, accumulate in the system.

Table 3
Meteoric water and serpentinite introduced in reaction path modelling (chemical composition of the meteoric water is modified from Berner and Berner 1996, that of the serpentinite is modified from Bruni and others 2001, 2002, and Angelone and others 1991)

Meteoric water (pH 5.5)		Serpentinite	
Component	Concentration (mg kg^{-1})	Element	Atomic fraction
Ca	0.29	Si	1.16E–01
Mg	0.45	Al	1.33E–03
Na	3.45	Fe	1.98E–02
K	0.17	Mn	3.02E–04
C (as HCO_3)	1.01	Mg	1.40E–01
SO_4	1.45	Ca	5.12E–03
Cl	6.00	Na	2.66E–04
NO_3	0.50	K	4.55E–04
NH_3	0.03	O	5.11E–01
SiO_2	7.5E–04	Cr	5.71E–05
Al	6.0E–07	Ni	5.62E–05
Cr	9.0E–08	H	2.04E–01
Fe	6.0E–07		
Mn	6.0E–08		
Ni	2.0E–07		

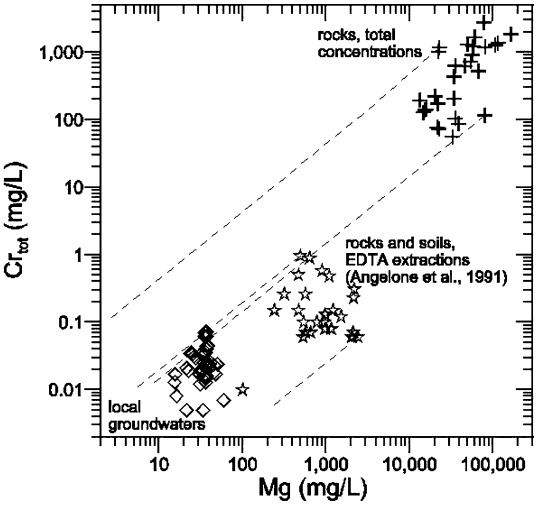

Fig. 6
Log-log plot of Cr vs. Mg, showing total concentrations in ultramafic rocks, concentrations in 0.05 M EDTA solutions at pH 7 after selective extraction from ultramafic rocks and related soils (Angelone and others 1991), and measured concentrations in groundwaters of the study area

The initial aqueous solution, external conditions, and possible product phases

The local meteoric water was assumed to be represented by the average meteoric water of coastal regions (Table 3, from Berner and Berner 1996). EQ3 was used to compute the total concentration of carbonate species by imposing the electroneutrality constraint, whereas pH was considered to be fixed by the average atmospheric P_{CO2} value of $10^{-3.5}$ bar. The concentrations of trace constituents were calculated by multiplying their average seawater concentrations (Berner and Berner 1996) by the ratio between the Cl concentration of meteoric water (6 ppm) and that of seawater (19,350 ppm). This is a reasonable approximation since rainwaters in coastal regions are virtually strongly diluted seawater (Appelo and Postma 1996).

The simulation was carried out in two steps. In the first step, the serpentinite was reacted with meteoric water at a constant temperature of 10 °C, and constant P_{CO2} of $10^{-3.5}$, $10^{-2.5}$, and 10^{-2} bar in separate runs. P_{O2} was fixed to 10^{-9} bar, to reproduce the Cr(VI) dominance in the shallow circuits hosting Mg–HCO_3 waters. In the second step the system was closed with respect to CO_2, temperature was maintained at 10 °C, but P_{O2} was decreased to $10^{-73.6}$ bar. These conditions reproduce those of the deep aquifers hosting the more evolved waters, such as those discharged by the Issel spring.

Although EQ6 is able to choose automatically the solid product phases, only the precipitation of minerals typically forming through weathering of serpentinites and ultramafic rocks under climatic conditions similar to those of the study area (see above) was permitted. These solid phases are gibbsite, brucite, kaolinite, sepiolite, hydromagnesite, nesquehonite, a solid mixture of trigonal carbonates (calcite, siderite, rhodochrosite, gaspeite), a solid mixture of Fe(III)-, Mn(III)-, Cr(III)-, Fe(II)-, Mn(II)-, and Ni-hydroxides, a solid mixture of Mg-, Ca-, Na-, K-, Fe(III)-, Mn(III)-, Cr(III)-, Fe(II)-, Mn(II)-, and Ni-montmorillonites, and a solid mixture of Mg-, Ca-, Na-, K-, Fe(III)-, Mn(III)-, Cr(III)-, Fe(II)-, Mn(II)-, and Ni-saponites. This choice was dictated by two reasons: to prevent the automatic separation of solid phases which are unlikely to form in the environments under study, and to avoid unwanted modeling complications. Ideal mixing was assumed in the solid state, since only this mixing model is supported by the software EQ3/6, version 7.2.

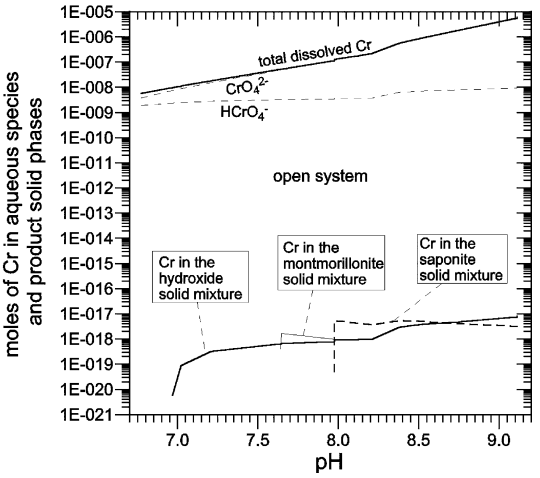

Fig. 8
Theoretical distribution of Cr in the aqueous phase and different solid sinks during the progressive dissolution of serpentinite under fixed P_{CO2} of $10^{-3.5}$ bar and P_{O2} of 10^{-9} bar

Results

A gradual increase in total dissolved Cr concentration is expected through progressive dissolution of serpentinite (Fig. 7) under open-system with CO_2 and at P_{O2} of 10^{-9} bar, as indicated by the results of the first simulation step. Computed data are in substantial agreement with analytical data. A decrease in total dissolved Cr concentration of 3–4 orders of magnitude is expected upon the decrease in P_{O2} from 10^{-9} to $10^{-73.6}$ bar, as suggested by the second simulation step. Unfortunately, no analytical data are available to confirm these low computed Cr concentrations, apart from the undetectable content (<5 ppb Cr) of the sulfide-bearing Issel spring, with a pH of 10.5.

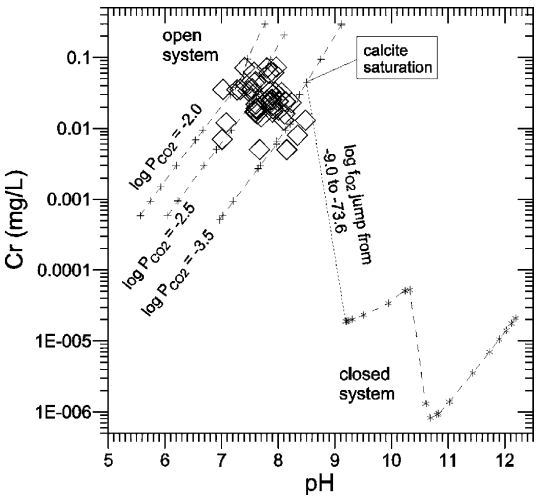

Fig. 7
Total dissolved Cr concentrations and pH values expected through progressive dissolution of serpentinite under different P_{CO2}, P_{O2} conditions (*curves*), and analytical Cr, pH values of Mg–HCO_3 waters (*diamonds*)

Based on the results of the first simulation step for P_{CO2} of $10^{-3.5}$ bar (Fig. 8), dissolved Cr is mainly represented by CrO_4^{2-} ion and subordinately by $HCrO_4^-$ ion, and the latter becomes progressively unimportant with increasing pH. The amounts of Cr incorporated in solid phases are 9–12 orders of magnitude lower than aqueous Cr contents, and are variably distributed between the solid mixtures of hydroxides, montmorillonites and saponites, depending on pH. Hydroxide represents the main solid reservoir of Cr below pH 7.6. It is substituted by montmorillonite between pH 7.6 and 8, and by saponite between pH 8 and 8.7. Above this pH value hydroxide becomes again the main solid sink of Cr, although the role of all these solids is completely negligible.

Under the reducing conditions of the second simulation step (P_{O2} $10^{-73.6}$ bar) Cr is mainly stored in the hydroxide solid mixture, subordinately in the aqueous phase, and in negligible amounts in saponite (Fig. 9a). Dissolved Cr is present in toto in the trivalent form, mainly as $Cr(OH)_4^-$ and secondarily as $Cr(OH)_3$.

Summing up, dissolved Cr(VI) is expected to persist in a stable form in the aqueous phase under the relatively oxidizing conditions of the shallow aquifers hosting Mg–HCO_3 and Ca–HCO_3 waters. Only the reducing substances present at greater depths, e.g., Fe(II) and organic matter, bring about the reduction of Cr(VI) to Cr(III), which is mainly sequestrated by precipitating hydroxides. Under all the investigated P_{O2}–P_{CO2}–temperature conditions, the amounts of Cr entering in montmorillonites and saponites are completely negligible.

Conclusions

Many waters of the study area have either Mg–HCO_3 or Ca–HCO_3 composition. Magnesium-rich waters are typically produced through limited interaction of meteoric

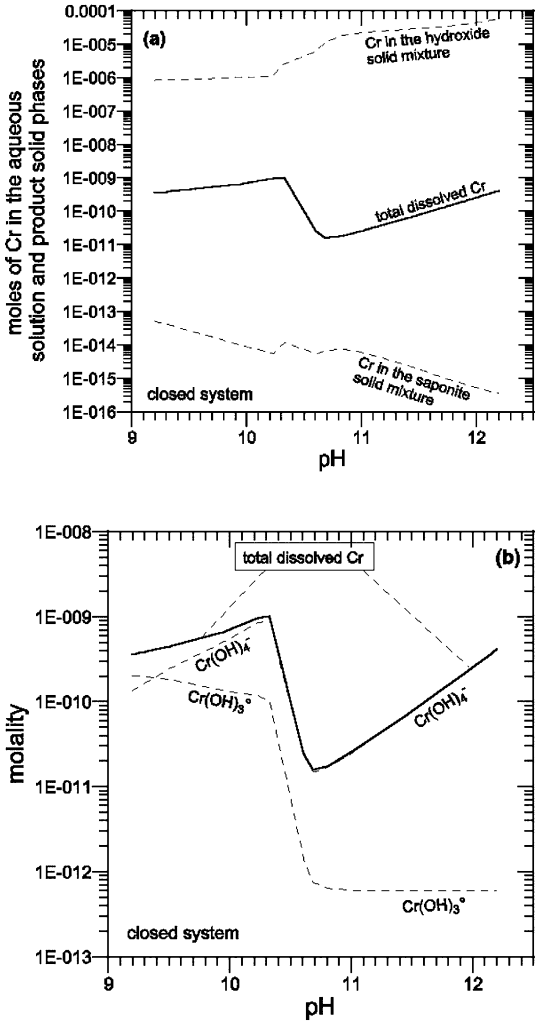

Fig. 9
a Theoretical distribution of Cr in different solid reservoirs and total dissolved Cr, and **b** theoretical speciation in the aqueous phase, during the progressive dissolution of serpentinite under P_{O2} of $10^{-73.6}$ bar and closed-system conditions with respect to CO_2

waters with serpentinites and ultramafic rocks, whereas Ca-rich waters originate through interaction of meteoric waters with gabbros and basalts. Only the sulfide-bearing Issel spring has peculiar characteristics, i.e., HCO_3–CO_3–OH–Na composition, a pH of 10.5, and an Eh of –0.3 V. It represents an intermediate product between immature Mg–HCO_3 waters and mature Ca–OH waters, which are generated through prolonged interaction of meteoric waters with serpentinites.

The Issel spring and 27 bicarbonate waters have undetectable Cr and Cr(VI), whereas 30 bicarbonate waters have nearly equal concentrations of Cr and Cr(VI). In these waters dissolved Cr is, therefore, present in toto in the hexavalent form, and Cr(VI) contents are above the maximum permissible level for drinking waters which is fixed at 5 ppb by the Italian regulations. Chromium concentrations of Mg–HCO_3 waters (maximum of 73 ppb) are usually higher than those of Ca–HCO_3 waters (up to 23 ppb). The distinct distributions of Cr in these two groundwater facies appear to be controlled, at least in part, by the different Cr contents of rocks (on average, 1,800 ppm for peridotites and 185 ppm for basalts) with which they come in contact.

Since Cr is present at the trivalent state in rock-forming minerals, the release of Cr to the aqueous solution requires oxidation of Cr(III) to Cr(VI), which can be carried out by different electron acceptors, including Mn-oxides, H_2O_2, gaseous O_2, and perhaps Fe(III) oxyhydroxides. Oxidation driven by atmospheric O_2 mimics the industrial process of chromite/sodium chromate conversion and could be effective during forest burning, which is rather common in the area under investigation.

The fate of Cr during water-rock interaction was investigated through reaction-path modeling. It turned out that aqueous Cr(VI) persists in a stable form in Mg–HCO_3 and Ca–HCO_3 waters, due to the relatively oxidizing conditions of the shallow environments in which these waters circulate. Only the electron donors encountered at depth, e.g., Fe(II) and organic matter, determine the reduction of Cr(VI) to Cr(III), which is chiefly sequestrated by precipitating hydroxides. Simulations also indicate that the amounts of Cr incorporated in montmorillonites and saponites are completely negligible under all the investigated P_{O2}–P_{CO2}–temperature conditions.

Acknowledgments This work would not have been possible without the support of ACAM and the help of Dr. Raffaele Peruzzi of ACAM, who is gratefully acknowledged by the authors.

References

Abbate E, Bortolotti V, Principi G (1980) Apennine ophiolites: a peculiar oceanic crust. In: Rocci G (ed) Tethyan ophiolites. Ofioliti Spec Issue 5:59–96

Angelone M, Vaselli O, Bini C, Coradossi N, Pancani MG (1991) Total and EDTA-extractable element contents in ophiolitic soils from Tuscany (Italy). Z Pflanzenernähr Bodenk 154:217–223

Appelo CAJ, Postma D (1996) Geochemistry, groundwaters and pollution. Balkema, Rotterdam

Barnes HL, Langmuir D (1978) Geochemical prospecting handbook for metals and associated elements. Natl Sci Foundation Grant no AER77-06511 AO2, Annu Rep

Barnes I, O'Neil JR (1969) The relationship between fluids in some fresh alpine-type ultramafics and possible modern serpentinization, western United States. Geol Soc Am Bull 80:1947–1960

Barret TJ (1982) Review of stratigraphic aspects of the ophiolitic rocks and pelagic sediments of Vara Complex, northern Apennine, Italy. Ofioliti 7:3–45

Berner EK, Berner RA (1996) Global environment. Water, air, and geochemical cycles. Prentice Hall, Upper Saddle River, NJ

Bini C, Vaselli O, Coradossi N, Pancani MG, Angelone M (1990a) Clay mineral formation from mafic rocks in temperate climate, central Italy. Sci Géol Bull 43:129–138

Bini C, Coradossi N, Vaselli O, Pancani MG, Angelone M (1990b) Weathering and soil mineral evolution from mafic rocks in temperate climate, central Italy. In: Trans14th Int Congr Soil Science, Kyoto, 1990, vol 7, pp 54–59

Bruni J, Canepa M, Cipolli F, Marini L, Ottonello G, Vetuschi Zuccolini M, Chiodini G, Cioni R, Longinelli A (2001) Reactions

governing the chemistry of waters interacting with serpentinites. In: Cidu R (ed) Proc 10th Water Rock Interaction Conf, Villasimius, 10–15 July 2001, vol 1. Balkema, Rotterdam, pp 145–148
Bruni J, Canepa M, Cipolli F, Marini L, Ottonello G, Vetuschi Zuccolini M, Chiodini G, Cioni R, Longinelli A (2002) Irreversible water-rock mass transfer accompanying the generation of the neutral, Mg-HCO_3 and high-pH, Ca-OH spring waters of the Genova province, Italy. Appl Geochem 17:455–474
Caillère S, Henin S (1949) Occurrence of sepiolite in the Lizard serpentines. Nature 163:962
Cortesogno L, Galbiati B, Principi G, Venturelli G (1978) Le brecce ofiolitiche della Liguria Orientale: nuovi dati e discussioni sui modelli paleogeografici. Ofioliti 3:99–160
Cortesogno L, Galbiati B, Principi G (1980) Le brecce serpentinitiche giurassiche della Liguria Orientale. Arch Sci Genève 33:185–200
Cortesogno L, Galbiati B, Principi G (1987) Note alla Carta geologica delle ofioliti del Bracco e ricostruzione della paleogeografia giurassico cretacica. Ofioliti 12:261–342
Cranston RE, Murray MJ (1978) The determination of chromium species in natural waters. Anal Chim Acta 99:275–282
Decandia FA, Elter P (1972) La zona ofiolitifera del Bracco nel settore compreso fra Levanto e la Val Graveglia (Appennino Ligure). Mem Soc Geol It XI:503–530
Deer WA, Howie RA, Zussman J (1975) An introduction to the rock-forming minerals. Longman, London
De Siena C, Vaselli O (1994) Pedological, mineralogical and geochemical investigations of ophiolitic soils from Lanciaia-Montecastelli Pisano (Tuscany-Italy). Mem Soc Geol It 48:675–680
Dinelli E, Lombini A, Simoni A, Ferrari C (1997) Heavy metals in serpentinite soils of selected outcrops of Piacenza and Parma provinces (Northern Apennines, Italy). Mineral Petrogr Acta 40:241–255
Eary LE, Rai D (1987) Kinetics of chromium (III) oxidation to chromium (VI) by reaction with manganese dioxide. Environ Sci Technol 21:1187–1193
Emerson S, Cranston RE, Liss PS (1979) Redox species in a reducing fjord: Equilibrium and kinetic considerations. Deep-Sea Res 26:859–878
Faure G (1992) Principles and applications of inorganic geochemistry. Maxwell-Macmillan, New York
Fendorf SE (1995) Surface reactions of chromium in soils and waters. Geoderma 67:55–71
Fendorf SE, Zasoski RJ (1992) Chromium (III) oxidation by δ-MnO_2. I. Characterization. Environ Sci Technol 26:79–85
Freyssinet P, Farah AS (2000) Geochemical mass balance and weathering rates of ultramafic schists in Amazonia. Chem Geol 170:133–151
Fukai RM, Vas D (1969) Changes in the chemical forms of chromium on the standing of seawater samples. J Oceanogr Soc Jpn 25:47–49
Helgeson HC (1979) Mass transfer among minerals and hydrothermal solutions. In: Barnes HL (ed) Geochemistry of hydrothermal ore deposits, Wiley, New York, pp 568–610
Hostetler PB, Coleman RG, Mumpton FA, Evans BW (1966) Brucite in alpine serpentinites. Am Mineral 51:75–98
Johnson CA, Xyla AG (1991) The oxidation of chromium (III) to chromium (VI) on the surface of manganate (γ-MnOOH). Geochim Cosmochim Acta 55:2861–2866
Johnson JW, Oelkers EH, Helgeson HC (1992) SUPCRT 92: A software package for calculating the standard molal thermodynamic properties of minerals, gases, aqueous species, and reactions from 1 to 5000 bars and 0 to 1000 °C. Comput Geosci 18:899–947
Lin FC, Clemency CV (1981) The dissolution kinetics of brucite, antigorite, talc, and phlogopite at room temperature and pressure. Am Mineral 66:801–806
Marini L, Ottonello G, Canepa M, Cipolli F (2000) Water-rock interaction in the Bisagno Valley (Genoa, Italy): application of an inverse approach to model spring water chemistry. Geochim Cosmochim Acta 64:2617–2635
Nriagu JO (1988) Production and uses of chromium. In: Nriagu JO, Niebner E (eds) Chromium in the natural and human environments. Wiley, New York, pp 81–104
Ottonello G (2001a) Convenzione ANPA-CNR finalizzata alla realizzazione di prototipi di carte tematiche di parte del territorio nazionale alla scala 1:250.000 riportanti i tenori naturali di alcuni elementi chimici di significativo impatto ambientale. DipTeRis, University of Genova
Ottonello G (2001b) The inverse modeling of water-rock interaction. In: Cidu R (ed) Proc 10th Water Rock Interaction Conf, Villasimius, 10–15 July 2001, vol 1. Balkema, Rotterdam, pp 47–60
Pettine M, Millero FJ (1990) Chromium speciation in seawater: the probable role of hydrogen peroxide. Limnol Oceanogr 35:730–736
Pfeifer H-R, Derron M-H, Rey D, Schlegel C, Atteia O, Dalla Piazza R, Dubois J-P, Mandia Y (1999) Natural trace element input to the soil-sediment-water-plant system: examples of background and contaminated situations in Switzerland, eastern France and northern Italy. In: Markert B, Friese K (eds) Trace metals in the environment 4. Elsevier, Amsterdam
Raphael MW, Boulis SN (1982) Kinetics of the oxidation of chromium (III) ions by trimanganese tetraoxide and by manganese (III) oxide. Surf Technol 16:243–248
Robles-Camacho J, Armienta MA (2000) Natural chromium contamination of groundwater at Leon Valley, Mexico. J Geochem Explor 68:167–181
Saleh FY, Parketon TF, Lewis RV, Huang JH, Dickson KL (1989) Kinetics of chromium transformations in the environment. Sci Total Environ 86:25–41
Schlegel C, Pfeifer HR (1999) Heavy metal contamination in soils, plants and waters in the vicinity of the peridotite massif of Baldissero-Canavese (N-Italy). In: Abstr Vol 2nd Conf Environmental Geochemical Baseline Mapping in Europe, Vilnius, 1–4 September 1999. Geologijos Institutas, Vilnius
Schroeder DC, Lee GF (1975) Potential transformations of chromium in natural waters. Water Air Soil Pollut 4:355–365
Steinmann G (1905) Geologische Beobachtungen in den Alpen. Ber Naturf Ges Freiburg 16:18–67
Suarez DL, Simunek J (1996) Solute transport modeling under variably saturated water flow conditions. In: Lichtner PC, Steefel CI, Oelkers EH (eds) Reactive transport in porous media. Rev Mineral 34:229–268
Suess E (1888) Das Antlitz der Erde, 2. G Freytag, Leipzig
Suess E (1901) Das Antlitz der Erde, 3(1). G Freytag, Leipzig
Sverjensky D (1984) Prediction of Gibbs free energies of calcite-type carbonates and the equilibrium distribution of trace elements between carbonates and aqueous solutions. Geochim Cosmochim Acta 48:1127–1134
Sverjensky D (1985) The distribution of divalent trace elements between sulfides, oxides, silicates and hydrothermal solutions. I. Thermodynamic basis. Geochim Cosmochim Acta 49:853–864
Svoboda-Goldberg NG, Drever JI (1992) Mineral dissolution rates in pilot-scale field and laboratory experiments. Chem Geol 105:51–69
Vaselli O, Bini C, Del Sette M (1993) Géochimie des eaux lessivantes un sol brun eutrophe (typic xerochrept) sous foret en climat tempéré. Quad Sci Suolo 5:75–89
Velbel MA (1993) Constancy of silicate-mineral weathering-rate ratios between natural and experimental weathering: Implication for hydrologic control of differences in absolute rates. Chem Geol 105:89–99

Venturelli G, Contini S, Bonazzi A, Mangia A (1997) Weathering of ultramafic rocks at Mt. Prinzera, northern Apennines, Italy. Mineral Mag 61:765–778
Wedepohl KH (1978) Handbook of geochemistry. Springer, Berlin Heidelberg New York
Wolery T (1992) EQ3NR, a computer program for geochemical aqueous speciation-solubility calculations: theoretical manual, user's guide and related documentation, version 7.0. Report UCRL-MA-110662 PT III, Lawrence Livermore National Laboratory, Livermore
Wolery T, Daveler SA (1992) EQ6, a computer program for reaction path modeling of aqueous geochemical systems: theoretical manual, user's guide, and related documentation, version 7.0. Report UCRL-MA-110662 PT IV, Lawrence Livermore National Laboratory, Livermore
Wollast R, Mackenzie FT, Bricker OP (1968) Experimental precipitation and genesis of sepiolite at earth-surface conditions. Am Mineral 53:1645–1661
Yamagata N, Murakami Y, Torii T (1960) Biogeochemical investigation in serpentine-chromite ore district. Geochim Cosmochim Acta 18:23
Yuan J, Shiller AM (2000) The variation of hydrogen peroxide in rainwater over the South and Central Atlantic Ocean. Atmos Environ 34:3973–3980